FACTA UNIVERSITATIS
Series: **Electronics and Energetics** Vol. 36, Nº 3, September 2023, pp. 411-426
https://doi.org/10.2298/FUEE2303411A

Original scientific paper

A CRITICAL REVIEW ON THE MATERIAL ASPECTS OF TRIBOELECTRIC NANOGENERATORS (TENG)

Deepak Anand, Ashish Singh Sambyal, Rakesh Vaid

Department of Electronics, University of Jammu, Jammu 180006, India

Abstract. *Triboelectric nanogenerators (TENG) take the advantage of coupling effect for harvesting energy in the area of electronics for various self-powered applications. These nanogenerators are capable of converting energy in our surroundings into electrical energy by using the process of electrostatic induction and contact electrification. Triboelectric layers of a TENG are formed basically with the use of various polymers, metals and other inorganic materials like PTFE (Poly tetra fluoro ethylene), PDMS (polydimethyl siloxane), FEP (Fluorinated ethylene propylene) and Kapton. Selection of different materials for the device fabrication is very important since it contribute towards the triboelectric effect and also forms the fundamental structure for the proposed TENG device. In this review article, we emphasis mainly on various triboelectric materials considering factors such as stability, flexibility, power density etc., to improve upon the electrical output of the devices for different applications.*

Key words: *TENG (Triboelectric Nanogenerator), PTFE (Poly tetra fluoro Ethylene), FEP (Fluorinated ethylene propylene), PDMS (Poly dimethyl siloxane), TET (triboelectric textile), PMMA (polymethyl methacrylate), Energy harvesting*

1. INTRODUCTION AND BACKGROUND

With the transport of electrons from one surface to another, Triboelectric nanogenerators (TENG) can be termed as significant devices for generating electrical output from ambient mechanical energy. Triboelectricity can be seen in our daily actions including walking, running, hand-to-hand contact, etc. [1-3] when charge separation on the surfaces that come into contact produces electrical potential and can be stored in energy storage units [4]. The TENG based devices can work in four modes such as vertical contact-separation [5-7], sliding [8-9], single electron [10-11], and free standing mode [12-13]. These devices use stretched materials as spacers [14–17] and also have arc-shaped structures [18] and are based on various models reported in the literature such as the band structure model [19],

Received January 24, 2023; revised April 01, 2023; accepted April 09, 2023
Corresponding author: Rakesh Vaid
Department of Electronics, University of Jammu, Jammu 180006, India
E-mail: rakeshvaid@ieee.org

molecular orbital model [20], and electron-cloud potential well model [21]. According to the band structure model, the movement of electrons is dependent on the energy disparity between the Fermi level of the metal and the valance band of the dielectric. This model does not work well when triboelectrification occurs between two dielectric materials which do not have well-developed band structures. The electron cloud potential well model states that the electrons have distinct energy levels where the electrons with a higher energy level tend to transfer from the other substance to the contacting atom. The molecular orbital model uses LUMO (lowest unoccupied molecular orbital) and HOMO (highest occupied molecular orbital) instead of using the conduction and valance bands as in case of semiconductor materials. Here, the electrons move as a result of the disparity in neutral levels between the surfaces of two dielectrics that are in touch. The method of electron transfer during the creation of tribolelectricity is still under investigation and depends on the selection of triboelectric materials according to various theories proposed so far. In this review paper, we have presented various material strategies to increase triboelectric power, triboelectric-series along with an analysis of the material selections for the different TENG structures investigated during the last decade.

2. Various Materials To Enhance Triboelectric Power

The progress in materials for the four representative component layers has been discussed in this section. The various layers are: the charge generating layer, the charge trapping layer, the charge collecting layer, and the charge storage layer as shown in Figure 1.

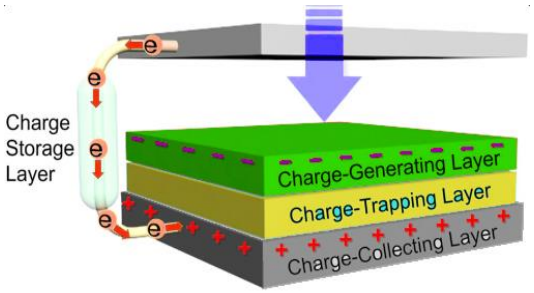

Fig. 1 Components of a TENG affecting triboelectric power generation [22]

2.1. Charge Generating Layer

The charge density of the contact surface and TENG performance are directly proportional to one another [23] and can be increased to boost the electric output power. The primary factor used to determine the figure of merit is the square of charge density [24]. Several strategies have been reported from the perspective of materials [25] and in each of these methods; the contact area is enhanced through the production of nanostructures to raise the surface charge density, or through the doping of surfaces to improve the triboelectric effect, or through the use of molecular synthesis to produce novel materials. A simple way to boost the overall charge created is to increase the contact surface area. Several techniques, such as force assembled colloidal arrays [26], lithography [27], anodic aluminum oxide [28], block-copolymer assembly [29], and surface nano material production [30–31], have been reported

for fabricating the microstructures. According to a recent study by Lee et al. [32], an increase in adhesion energy enhances the formation of surface charges, as can be seen in Figure 2 (a). PDMS (*Poly dimethyl siloxane)* is known to be a silicon-based organic polymer with the chemical formula CH_3 [Si $(CH_3)_2O$]n Si $(CH_3)_3$, having many chains which can be clearly seen from the FESEM images, where n is the number of repeating monomers [SiO $(CH_3)_2$] units. To prepare a solution of PDMS, the sylgard 184 elastomer and its curing agent are mixed thoroughly in 10:1 proportion and further to make the solution more dilute, 1 ml of methyl chloride can be added in the prepared solution and then is kept in vacuum for about 30 minutes to remove air bubbles. PDMS layer can be deposited on the surface of a substrate by spin coating where layers of different thickness can be deposited by varying rpm, time and acceleration. On the substrate, micro pillars of PDMS are created, and a PDMS film is employed to cover their top. The PDMS thin film stores the applied mechanical energy during the contact and separation processes due to its significant elastic deformation. As a result, more charge can be generated on adhesive surfaces than on the non-adhesive surfaces. Triboelectricity can be produced when two surfaces come into contact with different potentials, which supports the idea that one of the main components of sticky surfaces is fictionalization of the material surface.

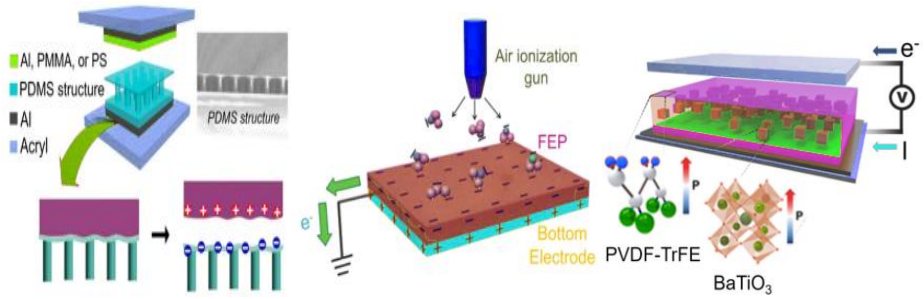

(a) (b) (c)

Fig. 2 Power enhancement of devices using charge generating layer (a) Increased output using pillar based structure [32]; (b) Ionized-air injection [33]; (c) Ferroelectric polarization and dielectric properties for boosting power [34]

The main techniques for altering the surfaces in contact are plasma treatment and ion-doping radical injection, and both these techniques have a considerable impact on charge creation [35–38]. The flow of electrons from aluminum surface to FEP [fluorinated ethylene propylene] surface increases when FEP is exposed to negatively ionized air [33] [see Figure 2 (b)]. A change in the intrinsic material properties, such as dielectric constant, polarity, work-function, etc., can be sought through the processes of nanocomposite formation, electrical poling, chemical doping, and material synthesis. Polyvinylidene fluoride-co-trifluoroethylene, one of the well-known ferroelectric polymers, can also be polarized utilizing an electrical poling procedure [39]. The positive triboelectric series suggested by Lee et al., [40] indicates that PVDF-TrFE after electrical poling outperformed on human skin. On electrical poling, the charge generation has been increased by about 18 times with PVDF-TrFE and high K barium titanate ($BaTiO_3$) nanoparticles as compared to pure PVDF-TrFE [41] as can be seen from Figure 2(c).

2.2. Charge Trapping Layer

In this section, we will present current developments in the materials to block the charge. Combination charge traps are produced by a variety of physical and chemical flaws, including dangling bonds, cross-linking sites, amorphous free volumes, and functional groups in the polymer chains [42–43]. Since their chains contain aromatic rings, several polymers, including polystyrene (PS) and polyimide (PI) have a lot of trapping sites [44]. When an aromatic interlayer is added between the PVDF layer and the collector electrode, the triboelectric output increases by about 7-9 times when compared to the device without an interlayer [45] as shown in Figure 3 (a). On the other hand, PDMS contains larger and deeper charge traps than aromatic polymers as can be seen from Figure 3 (b). The inclusion of a PDMS thin film beneath the charge-generating layer can boost the power density of TENG devices by more than 100 times. The addition of a PDMS layer further improves the device stretchability [46]. It has also been shown that the performance of a TENG [47] and its function as charge reservoir [48] can be significantly improved by the addition of Titanium Oxide (TiOx) and Indium Zinc Oxide (IZO) interlayers. When compared to thin film interlayers, more charge trapping can be achieved by using nanomaterials with greater surface-to-volume ratio. The power density of TENG devices can be increased by the monolayer of MoS_2 by acting as an electron acceptor [49]. Similar to this, composites made up of reduced Graphene Oxide nanosheets can effectively trap electrons by improving output performance [50]. In order to create the high performance textile TENG as depicted in Figure 3 (c), paintable and coatable

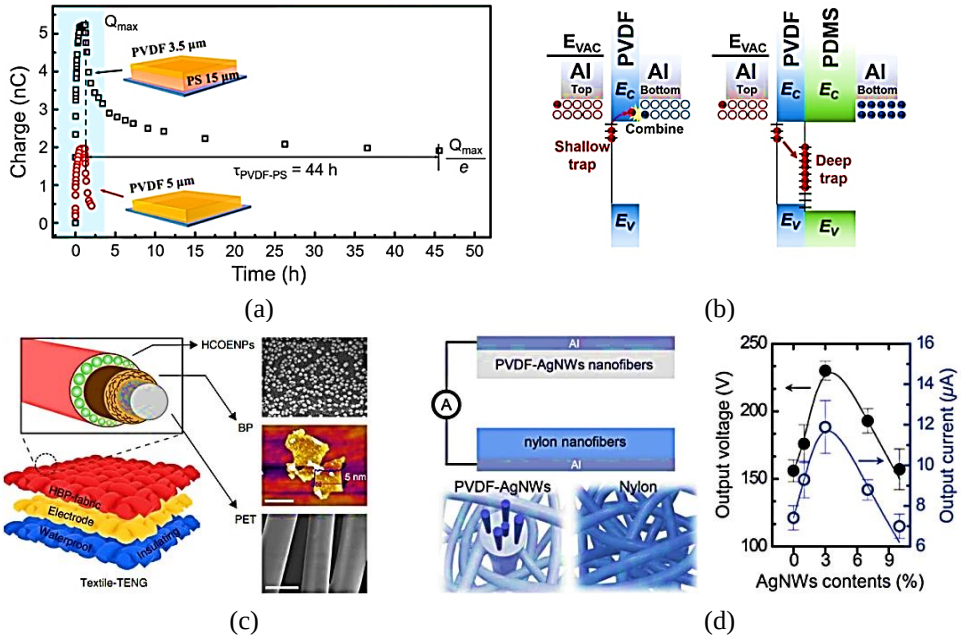

Fig. 3 Power enhancement using charge trapping layer (a) Trapping of Triboelectric charges with/without the PS dielectric interlayer [45]; (b) Mechanism of trapping charge with a PDMS layer [46]; (c) Trapping of electrons using black phosphorous layer coated with hydrophobic nanoparticles [51]; (d) Increasing of charge trapping and charge induction by using silver nanowires [52]

composites of black phosphorous (BP) ornamented or coated with hydrophobic cellulose oleoyl ester nanoparticles are being used as an electron trapping ingredient. In case of PVDF nanofibers, formation of a β-Crystalline phase in the PVDF chains takes place by the addition of silver nanowires (AgNW's) resulted in the induction of charge trapped at the metal-dielectric interface. This process increases the output performance of TENG devices [52] as demonstrated in the Figure 3 (d). Because of synergetic effects by incorporating nanocrystals of metal organic frameworks (MOFs) [53] and Titania monolayer ($Ti_{0\text{-}87}O_2$) [54] into the charge generating layer, there can be an increase in the total output power of a TENG device.

2.3. Charge Collecting Layer

When two dielectric surfaces come into contact with one another, the generated charges are propelled electrostatically to flow from one electrode to the other. When an electrode makes contact with a dielectric, it simultaneously acts as a charge-generating layer and a charge-collection layer [35]. Metals [55] Graphene [56] and ITO [57] are just a few examples of the stiff and flexible electrodes that have been used during the fabrication process. The methods used to create deformable electrodes and their applications in stretchy TENG are covered in this section. Most stretchy devices [58–62] use buckling electrodes and in-plane serpentine metal extensively. Such wavy metal electrode can't be used in the fabrication of TENG devices due to the enormous dimensions and application of significant mechanical force. Alternative to these electrodes are the conductive elastic nanocomposites because they have a very low cost of printing and highly stable under repeated mechanical impacts and frictions [63-65]. To fabricate deformable TENG devices [66-67], composites made up of metal (Au) nanosheets are embedded in a PDMS matrix thus used as a charge collecting layer in TENG structure (refer Figure 4 (a) [68]). As shown in Figure 4 (b), the output voltage has

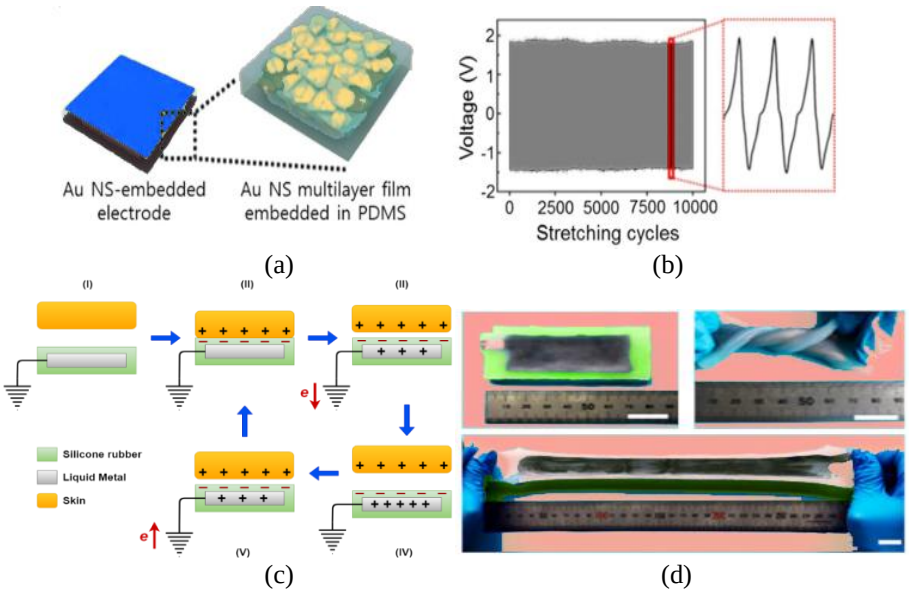

Fig. 4 Charge collection using stretchable materials (a) Stretchable electrode made by embedded gold nanosheets in the PDMS matrix; (b) Voltage output by applying cyclic elongation strain [68]; (c) Working of device using a liquid metal electrode; (d) A high stretchable device [72]

been maintained constant for elongation strain (30%) across 10,000 iterative cycles. Liquid metals can also be used for very stretchy electrodes [69–71] due to the fluidic nature of elastomeric matrix and can be injected into a tiny channel created in it at room temperature as shown in Figure 4 (c). A single electrode TENG [72] as depicted in Figure 4 (d) is highly stretchable and malleable without rupturing the electrode. Stretchable charge collectors for a TENG has been created by combining (PEDOT:PSS), or Poly (3.4-ethylene dioxythiophene): Poly (styrene sulfonate), with physiological saline, one of the liquid state conducting polymers [73-74].

2.4. Charge Storage Layer

Electricity generated by a TENG can be used in the form of a power supply by employing a capacitor and a bridge rectifier circuit for converting AC into DC [75] and by installing a rechargeable battery at its output terminals as demonstrated by Nun et al. where high conversion efficiency has been reported for a TENG with the use of a Lithium ion battery (LIB) [76] as shown in Figure 5 (a). For triboelectric energy charging, various materials have been utilized which includes $Li_3V_2(PO_4)_3$ [76], $LiFePO_4$ (LFP) [77-78], $LiMn_2O_4$ (LMO) [79] and $LiCoO_2$ (LCO) [80] and provide a very high efficiency of the order of ~ 80%. Li-ion battery requires a current in milli-amperes (mA) range for charging and discharging [80] and need a coil transformer with high amplitude output AC current. However, the direct charging of a battery is not possible due to very low current density to overcome the charging energy barrier. Thus the energy output of a TENG can be stored in capacitors and can be fabricated by inserting a dielectric layer between two electrodes. The dielectric capacitance is expressed as:

$$C = K\varepsilon_0 A / d \tag{1}$$

where, K = Dielectric constant, ε_0 = Vacuum permittivity, A = Electrode area and d = Dielectric thickness.

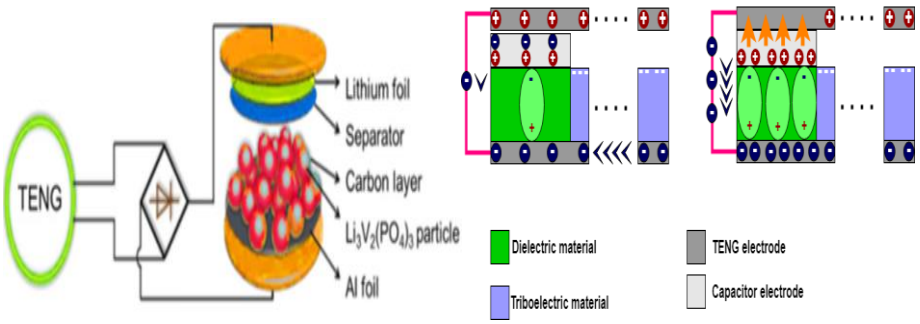

(a) (b)

Fig. 5 Storing charge in TENG: (a) Combination of TENG and LIBs based on $Li_3V_2(PO_4)_3$/C nanocomposites [76]; (b) Dielectric with a PVDF-TrFE used for storing and releasing the electrostatic charges [84]

The performance of a capacitor is characterized by its dimensions and inherent permittivity. To achieve a high-power density; fast charging and discharging, inorganic dielectric materials can be utilized. Since these inorganic dielectric film capacitors have very poor flexibility; the growth of dielectric materials on metal foils as well as on flexible organic substrates has been investigated [81-82]. Liang et al. has grown a film of ITO on Fluorophlogopite (FMica) and can be used as a bendable and a high temperature resistant to grow a BZT [Barium Zinc Titanate] layer of dielectric on ITO [83]. A capacitor integrated TENG was reported by Chung et al. in which PVDF-TrFE was used for storing electrostatic charge released due to Leyden jar effect [84] as shown in Fig. 5 (b) which clearly indicates that the charging of dielectric layer (green) takes place through the triboelectric layer (blue) in between a TENG electrode (gray) and a capacitor electrode (light gray). A large current (~4.3mA) was generated when the metal comes in contact with TENG electrode and the metal to metal contact released the stored charges.

3. TRIBOELECTRIC SERIES

After going through a triboelectrification process using a reference material, the surface charge density of the materials determines their triboelectric effects. Triboelectrification can be based on sliding or contact separation processes. Same materials with different triboelectrification have different surface charge densities. PTFE is the most frequently used triboelectric material in current TENG experiments due to its high electron-accepting capabilities. Based on the affinity to electrons, various materials are arranged in a series in which the materials are having different charge densities after the triboelectrification process. The first triboelectric series was published in 1757 by Swedish physicist Johan Carl [85]. At the Georgia Institute of Technology, Wang's team in 2019 created a novel technique [86] that could measure the triboelectric charge densities (TECD) of various materials using mercury-based triboelectrification in the contact separation mode. Based on TECDs of materials, a new series was developed which is more reliable because of precise control over electrification process. With quantified charge densities, another triboelectric series [87] was developed based on sliding mode. One of the most important parameters that influences the output of a TENG is the displacement current which is totally different from the displacement current represented by Maxwell equations. The electric displacement vector in Maxwell equations is represented as, $D = \varepsilon_0 E + P$ where E = Electric field and P = Polarization vector.

The surface charges that are generated in a TENG are independent of the external electric field [88]. This in case of TENG a new term needs to be added and hence the displacement vector can be rewritten as:

$$D = \varepsilon_0 \mathrm{E} + \mathrm{P} + \mathrm{P_s} \tag{2}$$

The expression for displacement current density in case of TENG is written as:

$$\mathrm{J_D} = \frac{\partial D}{\partial T} + \frac{\partial P_s}{\partial T} = \varepsilon_0 \frac{\partial E}{\partial T} + \frac{\partial P_s}{\partial T} \tag{3}$$

In case of a short circuit the current density can be written as: [89]

$$J_D = \alpha_T \frac{dH}{dt} d_1 \frac{\varepsilon_0}{\varepsilon_1} + d_2 \frac{\varepsilon_0}{\varepsilon_2} \frac{1}{(d_1 \frac{\varepsilon_0}{\varepsilon_1} + d_2 \frac{\varepsilon_0}{\varepsilon_2} + Z)^2} + \frac{d\alpha_T}{dt} H \frac{1}{(d_1 \frac{\varepsilon_0}{\varepsilon_1} + d_2 \frac{\varepsilon_0}{\varepsilon_2} + Z)^2} \quad (4)$$

where α_T = Surface charge density, H = Function of time, dH / dT = Contact-separation of two media in TENG, d_1, d_2 = Thickness of two media, ε_0 = Vacuum permittivity, ε_1 and ε_2 = Permittivity of two media, Z = Gap between two triboelectric layers.

When the surface charge density built up after few cycles the second term in equation (4) becomes negligibly small and hence can be neglected. This equation (4) can be written as:

$$J_D \approx \alpha_T \frac{dH}{dt} d_1 \frac{\varepsilon_0}{\varepsilon_1} + d_2 \frac{\varepsilon_0}{\varepsilon_2} \frac{1}{(d_1 \frac{\varepsilon_0}{\varepsilon_1} + d_2 \frac{\varepsilon_0}{\varepsilon_2} + Z)^2} \quad (5)$$

The output current "I" of a TENG can be represented as:

$$J_D = \mathrm{I} / \mathrm{A}, \mathrm{I} \approx \mathrm{A}.J_D \quad (6)$$

$$\mathrm{I} \approx \mathrm{A}.\alpha_T \frac{dH}{dt} d_1 \frac{\varepsilon_0}{\varepsilon_1} + d_2 \frac{\varepsilon_0}{\varepsilon_2} \frac{1}{(d_1 \frac{\varepsilon_0}{\varepsilon_1} + d_2 \frac{\varepsilon_0}{\varepsilon_2} + Z)^2} \quad (7)$$

4. CHOICE OF MATERIALS FOR A TENG

Triboelectrification depends on the movement of electrons between two materials that are in close proximity to one another. The ability of two materials to transport electrons between one another is determined by their electron affinities. Higher electron-affinity material will draw electrons and thus act as an electron donor. The material is electron donor or, electron acceptor depends upon its position in the triboelectric series. In this section, summary of various materials has been mentioned on random basis. Figure 6 shows various materials acting as electron acceptors and electron donors respectively. A total of fourteen different materials acting as electron acceptor and a total of 20 different materials acts as electron donor. The most popular materials for creating triboelectric layers and electrodes are Al, Cu, Ag, and Au. Figure 7 depicts the networking that occurs when electron acceptors and donors from various articles are paired. 14 donors are partnered with PTFE, 10 donors with PDMS, 6 donors with FEP, and 14 donors with Kapton. The materials used as 4, 3, and 2 donors are PET, silicone, polystyrene (PS), and cellulose respectively. The most extensively utilized triboelectric materials are PTFE, PDMS, and FEP because they have a high electron attracting affinity and therefore more negative materials. In contrast, Kapton, PET, and silicone are less common since they have a low electron attracting affinity.

Recently cellulose materials have drawn attention due to their capacity for mass production and sustainability. TENG have been made using a variety of cellulose materials, including nano and micro cellulose [89–90], regenerated cellulose, and modified cellulose [91]. Because they have a more transparent mechanism than other polymers, several inorganic materials like graphene [92], MoS_2 [93], and WS_2 [94] have also been employed in the fabrication of TENG. Specific material selections based on low coefficients of friction and high electron acceptivity, PTFE and FEP are the materials that are most frequently employed

for lateral sliding mode and freestanding triboelectric layer mode. Many other pairs such as PTFE – nylon [95], PTFE-Al [96-97], FEP-Cu [98 -99] and PTFE-skin [100] are used for lateral sliding mode and freestanding triboelectric layer because of their low co-efficient of friction. The commercialized application of TENG involves building of ultrasensitive sensors, micro-electromechanical devices, self powered systems, wearable electronics etc. to meet the high energy requirements.

4.1. Material Choice Evaluation for TENG

One of the most important factors for selecting a pair of triboelectric material is the difference in their charge affinity which ultimately depends upon the separation of materials in the triboelectric series i.e., how far the two materials are from each other. If this principle is followed then PTFE-Nylon is one of the best pairs for TENG fabrication. There are also many other factors that influence the output performance of TENG devices. This can be explained clearly from the equation as under:

$$P_1 = \alpha_T$$
$$P_2 = \frac{dH}{dt} \tag{8}$$
$$P_3 = d_1\frac{\varepsilon_0}{\varepsilon_1} + d_2\frac{\varepsilon_0}{\varepsilon_2}\frac{1}{(d_1\frac{\varepsilon_0}{\varepsilon_1} + d_2\frac{\varepsilon_0}{\varepsilon_2} + Z)^2}$$

The first Part P_1 of equation (8) is the surface charge density α_T which depends upon various factors such as materials chemical composition, elasticity in case of contact separation mode and co-efficient of friction in case of sliding and freestanding triboelectric layer mode. Part P_2 represents dH/dT which describes the rate/ speed of contact-separation and sliding in case of these two modes of operation. Electrostatic induction is the third part represented by P_3. In this part, the main impact is of permittivity on the induced charge on the back electrodes.

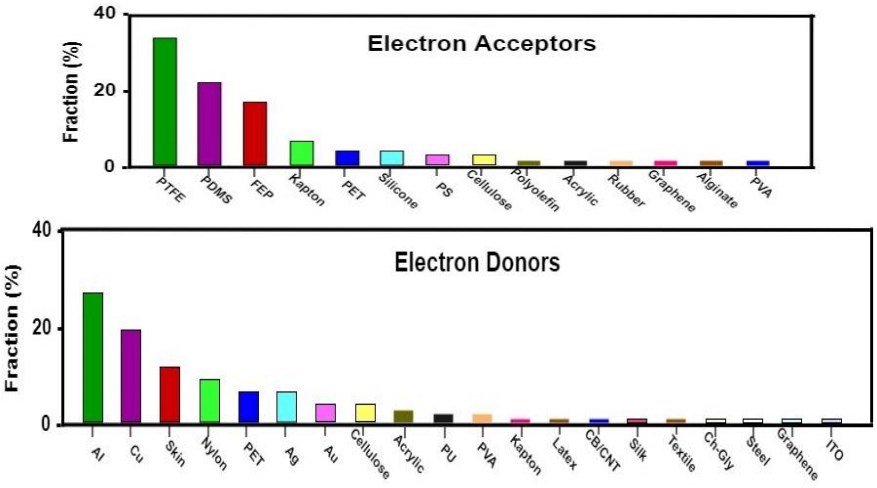

Fig. 6 Fraction (%) of the electron acceptor and donor materials

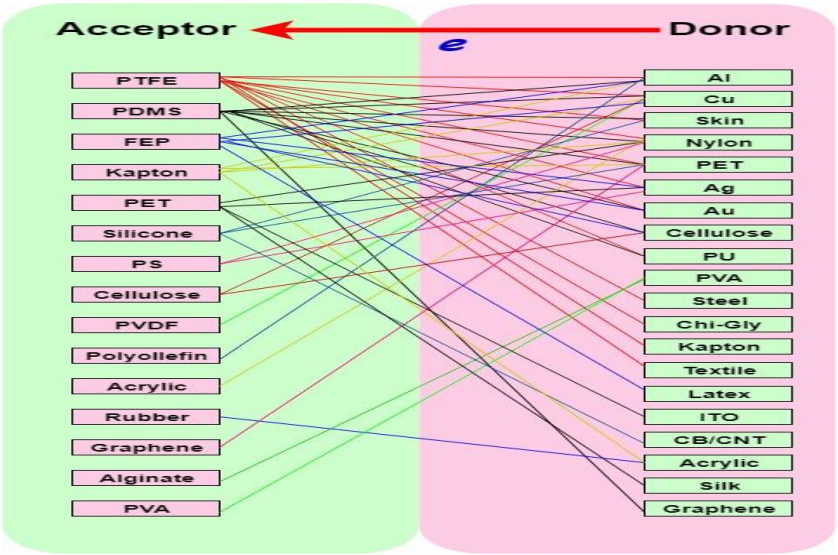

Fig. 7 Pairing of electron acceptor and donors

4.2. Donor of Electrons

4.2.1. Metals

In case of metals, the term $d_2(\varepsilon_0/\varepsilon_2)$ is Zero because $d_2 = 0$, that's why metals are widely used for fabricating TENG devices. Thus the current density J_D can be reduced as:

$$J_D \approx \alpha_T \frac{dH}{dt} d_1 \frac{\varepsilon_0}{\varepsilon_1} + d_2 \frac{\varepsilon_0}{\varepsilon_2} \frac{1}{(d_1 \frac{\varepsilon_0}{\varepsilon_1} + Z)^2} \tag{9}$$

and, equation (9) can be rewritten as:

$$P'_3 = d_1 \frac{\varepsilon_0}{\varepsilon_1} + d_2 \frac{\varepsilon_0}{\varepsilon_2} \frac{1}{(d_1 \frac{\varepsilon_0}{\varepsilon_1} + Z)^2} \tag{10}$$

Equation (9) still works even if we assume that there is a thin layer of triboelectric material on the surface of metal. It is because the metals have very high relative permittivity as in case of copper the value of relative permittivity is as high as > 250,000 with such a high value the term $d_2(\varepsilon_0/\varepsilon_2) = 0$, thus equation (10) is still valid.

When different metals are used as electron donors, the plots of the value of P'_3 in equation (10) for various materials versus the gap distance are shown in Figure 9 (a), whereas Figure 9 (b) shows the plots of the value in equation (8) versus the gap distance for various material pairs using PTFE as the electron acceptor. According to the above plotted data, those metals are ideally utilized as electron donors in pairs of triboelectric materials based on electrostatic induction. However, as depicted in Figure 8, electrostatic induction is the only one component of current density, and it is yet unknown about how big contribution it makes.

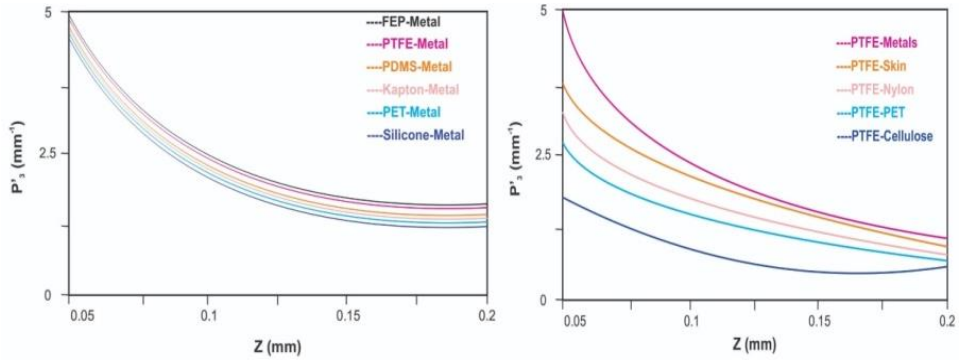

(a) (b)

Fig. 9 (a) Variations of P'_3 for different metals used as electron donors, 9 (b) shows the variations of P_3 using PTEE as the electron acceptor

4.2.2. Acceptors of Electrons

The popularly used materials that act as electron acceptors are PTFE [101], FEP [102] and PDMS [103]. Many studies done on polymers suggests that their output performance is very low because they show very less triboelectric effects against most commonly used electron donors. Triboelectric effect of such polymers is not strong against Mercury used TECD. PET has an extremely low TECD value of 101.48 μc/m^2 against Mercury, which is close to PTFE's -113.06 μc/m^2. Another test indicated that PET's charge density was 1.09 μc/m^2, which is significantly lower than PTFE as -27.5 μc/m^2 where PET was laterally dragged across a copper board. According to Fig. 8, P1 stands for the surface charge density T, which causes the triboelectric effect and depends on a number of factors, including the affinity of the charge, interaction between the several triboelectric layers, mode of operation or interaction, mechanical qualities, surface geometry, etc. The various materials used for TENG fabrication along with their output parameters are shown below in Table 1.

Table 1 Variations of various parameters with different triboelectric materials [104]

Positively Charged Materials	Negatively ChargedMaterials	Working Mode	Output Power (mW/cm^2)	Charge Density (μC/m^2)
PET	Kapton	Vertical-contact	0.00036	-
PET	PDMS	Vertical-contact	0.00234	-
Al	PDMS	Vertical-contact	3.56	-
Au	PDMS	Vertical-contact	31.3	594.2
Nylon	PTFE	Lateral-sliding	0.53	59
Al	FEP	Vertical-contact	31.5	240
Al	PVDF	Vertical-contact	0.26	360.2
Cu	PTFE	Freestanding	50	323
Al	ZnSnO3-PVDF (composites)	Vertical-contact	3	101.3
Cu	Kapton	Lateral-sliding	13.2	-
Al	PDMS	Vertical-contact	46.8	270
Al	PVDF-Gn	Vertical-contact	2.6	23

5. CONCLUSION

The usage of various materials in the fabrication of TENG devices is due to the phenomenon of triboelectrification that occurs at the interface when two triboelectric materials come into physical contact with each other. A number of materials have been tested and used in TENG fabrication amongst which Fluoro-polymers such as PTFE and FEP are the most widely used materials utilizing the free standing triboelectric and lateral sliding modes. These materials are the most commonly used electron acceptors whereas the most commonly used electron donors are Aluminum and Copper and has been explained quantitatively by using the recently developed equations which clearly indicates an increase in the electrostatic induction with the use of metals. Although, the selection of various materials for a particular TENG device has been investigated still many materials remained unexplored such as various green and functionalized materials, inorganic and composite materials. This review paper summarized the various material choices along with different types of triboelectric pairs that could be employed to contribute optimized displacement current density J_D for TENG structures. The paper further highlighted various material combinations those have been tested for charge generation, charge trapping, and charge collecting and the corresponding outputs of triboelectric nanogenerators.

Acknowledgement: *The author Deepak Anand and Ashish Sambyal organized the concept of this review paper and would like to thank Prof. Rakesh Vaid for supervising the project. All the authors read and approved the final manuscript.*

REFERENCES

[1] X. Cao, Y. Jie and Z. L. Wang, "Triboelectric nanogenerators driven self- powered electrochemical processes for energy and environmental science", *Adv. Energy Mater*. vol. 6, p. 1600665, 2016.
[2] S. H. Kwon et al., "Fabric active transducer stimulated by water motion for self-powered wearable device", *ACS Appl. Mater. Interfaces*, vol. 8, pp. 24579-24584, 2016.
[3] S. H. Wang, L. Lin and Z. L. Wang, "Triboelectric nanogenerators as self-powered active sensors", *Nano Energy*, vol. 11, pp. 436-462, 2015.
[4] C. S. Wu, A. C. Wang, W. B. Ding, H. Y. Guo and Z. L. Wang, "Triboelectric nanogenerator: a foundation of the energy for the new era", *Adv. Energy Mater*. vol.9, p. 1802906, 2019.
[5] S. M. Niu et al., "Theoretical study of contact-mode triboelectric nanogenerators as an effective power source", *Energy Environ. Sci*., vol. 6, pp. 3576-3583, 2013.
[6] H. L. Zhang et al., "Triboelectric nanogenerator built inside clothes for self-powered glucose biosensors", *Nano Energy*, vol.2, pp. 1019-1024, 2013.
[7] B. Yang et al., "A fully verified theoretical analysis of contact-mode triboelectric nanogenerators as a wearable power source", *Adv. Energy Mater*, vol. 6, p. 1600505, 2016.
[8] S. M. Niu et al., "Theory of sliding-mode triboelectric nanogenerators", *Adv. Mater*. vol. 25, pp. 6184-6193, 2013.
[9] G. Zhu et al., "A shape-adaptive thin film based approach for 50% high efficiency energy generation through micro-grating sliding electrification", *Adv. Mater*., vol. 26, pp. 3788-3796, 2014.
[10] B. Meng et al., "A transparent single-friction-surface triboelectric generator and self-powered touch sensor", *Energy Environ. Sci*., vol. 6, pp. 3235-3240, 2013.
[11] S. W. Chen et al., "An ultrathin flexible single-electrode triboelectric nanogenerator for mechanical energy harvesting and instantaneous force sensing", *Adv. Energy Mater*. vol. 7, p. 1601255, 2017.
[12] T. Zhou et al., "Woven structured triboelectric nanogenerator for wearable devices", *ACS Appl. Mater. Interfaces*, vol. 6, pp.14695-14701, 2014.
[13] Z. F. Zhao et al., "Freestanding flag-type triboelectric nanogenerator for harvesting high-altitude wind energy from arbitrary directions", *ACS Nano*, vol. 10, pp.1780-1787, 2016.

[14] Q. Zheng et al., "In vivo powering of pacemaker by breathing-driven implanted triboelectric nanogenerator", *Adv. Mater*., vol. 26, pp. 5851-5856, 2014.
[15] Y. H. Ko, S. H. Lee, J. W. Leem and J. S. Ju, "High transparency and triboelectric charge generation properties of nano-patterned PDMS", *RSC Adv*., vol. 4, pp. 10216-10220, 2014.
[16] F. R. Fan et al., "Highly transparent and flexible triboelectric nanogenerators: performance improvements and fundamental mechanisms", *J. Mater. Chem. A*., vol. 2, pp. 13219-13225, 2014.
[17] S. Kim et al., "Transparent flexible graphene triboelectric nanogenerators", *Adv. Mater*., vol. 26, pp. 3918-3925 2014.
[18] X. S. Zhang et al., "Frequency-multiplication high-output triboelectric nanogenerator for sustainably powering biomedical Microsystems", *Nano Lett*., vol. 13, pp. 1168-1172, 2013.
[19] Y. S. Zhou, S. Wang, Y. Yang, et al., "Manipulating Nanoscale contact electrification by an applied electric field", *Nano Lett*., vol. 14, pp. 1567-1572, 2014.
[20] C. Xu, B. Zhang, A. C. Wang, et al., "Contact-electrification between two identical materials: curvature effect", *ACS Nano.* vol. 13, pp. 2034-2041, 2019.
[21] C. Xu, A. C. Wang, H. Zou, et al., "Raising the working temperature of a triboelectric nanogenerator by quenching down electron thermionic emission in contact-electrification", *Adv Mater.*, vol. 30, p. 1803968, 2018.
[22] D. W. Kim, J. H. Lee, J. K. Kim, and U. Jeong, "Material aspects of triboelectric energy generation and sensors", *NPG Asia. Mater.*, vol. 12, pp. 1-17, p. 074103, 2020.
[23] S. M. Niu and Z. L. Wang, "Theoretical systems of triboelectric nanogenerators", *Nano Energy*, vol. 14, pp.161-192, 2015.
[24] Y. L. Zi et al., "Standards and figure-of-merits for quantifying the performance of triboelectric nanogenerators", *Nat. Commun*., vol. 6, p. 8376, 2015.
[25] D. Jang et al., "Force assembled triboelectric nanogenerator with high humidity resistant electricity generation using hierarchical surface morphology", *Nano Energy*, vol. 20, pp. 283-293, 2016.
[26] M. L. Seol et al., "Nature replicated nano in microstructures for triboelectric energy harvesting", *Small*, vol. 10, pp.3887-3894, 2014.
[27] C. K. Jeong et al., "Topographically-designed triboelectric nanogenerator via block co polymer self-assembly", *Nano Lett*. vol. 14, pp. 7031-7038, 2014.
[28] G. Zhu et al., "Triboelectric generator driven pulse electro deposition for micro patterning", *Nano Lett*. vol. 12, pp. 4960-4965, 2012.
[29] Z. H. Lin et al., "Enhanced triboelectric nanogenerators and triboelectric nanosensor using chemically modified TiO_2 nanomaterials", *ACS Nano*, vol. 7, pp. 4554-4560, 2013.
[30] J. H. Lee, I. Yu, S. Hyun, J. K. Kim and U. Jeong, "Remarkable increase in triboelectrification by enhancing the conformable contact and adhesion energy with a film-covered pillar structure", *Nano Energy*, vol. 34, pp. 233-241, 2017.
[31] J. Nie et al., "Power generation from the interaction of a liquid droplet and a liquid membrane", *Nat. Commun*., vol. 10, p. 2264, 2019.
[32] W. Seung et al., "Boosting power-generating performance of triboelectric nanogenerators via artificial control of ferroelectric polarization and dielectric properties", *Adv. Energy Mater*., vol. 7, p. 1600988, 2017.
[33] S. H. Wang et al., "Maximum surface charge density for triboelectric nanogenerators achieved by ionized-air injection: Methodology and theoretical understanding", *Adv. Mater*., vol. 26, pp. 6720-6728, 2014.
[34] B. K. Yun et al., "Base-treated polydimethylsiloxane surfaces as enhanced triboelectric nanogenerators", *Nano Energy*, vol. 15, pp. 523-529, 2015.
[35] X. S. Zhang et al., "High-performance triboelectric nanogenerator with enhanced energy density based on single-step fluorocarbon plasma treatment", *Nano Energy*, vol. 4, pp. 123-131, 2014.
[36] H. Y. Li et al., "Significant enhancement of triboelectric charge density by fluorinated surface modification in nanoscale for converting mechanical energy", *Adv. Funct. Mater*., vol. 25, pp. 5691-5697, 2015.
[37] P. H. Ducrot, I. Dufour and C. Ayela, "Optimization of PVDF-TrFE processing conditions for the fabrication of organic MEMS resonators", *Sci. Rep*., vol. 6, p. 19426, 2016.
[38] J. H. Lee et al., "Control of skin potential by triboelectrification with ferro-electric polymers", *Adv. Mater.*, vol. 27, pp. 5553-5558, 2015.
[39] W. Seung et al., "Boosting power-generating performance of triboelectric nanogenerators via artificial control of ferroelectric polarization and dielectric properties", *Adv. Energy Mater*., vol. 7, p. 1600988, 2017.
[40] W. W. Shen, B. Muh, G. J. Zhang, J. B. Deng and D. M. Tu, "Identification of electron and hole trap based on isothermal surface potential decay model", *J. Appl. Phys*., vol. 113, p. 083706, 2013.
[41] J. Y. Li, F. S. Zhou, D. M. Min, S. T. Li and R. Xia, "The energy distribution of trapped charges in polymers based on isothermal surface potential decay model", *IEEE Trans. Dielectr. Electr. Insul*., vol. 22, pp. 1723-1732, 2015.

[42] T. Takada et al., "Determination of charge-trapping sites in saturated and aromatic polymers by quantum chemical calculation", *IEEE Trans. Dielectr. Electr. Insul*., vol. 22, pp. 1240-1249, 2015.
[43] N. Y. Cui et al., "Dynamic behavior of the triboelectric charges and structural optimization of the friction layer for a triboelectric nanogenerator", *ACS Nano*, vol. 10, pp. 6131-6138, 2016.
[44] D. W. Kim, J. H. Lee, I. You, J. K. Kim and U. Jeong, "Adding a stretchable deep- trap interlayer for high-performance stretchable triboelectric nanogenerators", *Nano Energy*, vol. 50, pp. 192-200, 2018.
[45] H. W. Park et al., "Electron blocking layer-based interfacial design for highly- enhanced triboelectric nanogenerators", *Nano Energy*, vol. 50, pp. 9-15, 2018.
[46] D. Park, S. Lee, C. V. Anh, P. Park and J. Nah, "Role of a buried indium zinc oxide layer in the performance enhancement of triboelectric nanogenerators", *Nano Energy*, vol. 55, pp. 501-505, 2019.
[47] C. Wu et al., "Enhanced triboelectric nanogenerators based on MoS2 monolayer nano composites acting as electron-acceptor layers", *ACS Nano*, vol. 11, pp. 8356-8363, 2017.
[48] C. Wu, T. W. Kim and H. Y. Choi, "Reduced graphene-oxide acting as electron- trapping sites in the friction layer for giant triboelectric enhancement", *Nano Energy*, vol. 32, pp. 542-550, 2017.
[49] J. Q. Xiong et al., "Skin touch actuated textile based triboelectric nanogenerator with black phosphorus for durable biomechanical energy harvesting", *Nat. Commun*., vol. 9, p. 4280, 2018.
[50] S. Cheon et al., "High-performance triboelectric nanogenerators based on electro spun poly vinylidene fluoride-silver nanowire composite nanofibers", *Adv. Funct. Mater*., vol. 28, p. 1703778, 2018.
[51] R. M. Wen, J. M. Guo, A. F. Yu, J. Y. Zhai and Z. L. Wang, "Humidity-resistive triboelectric nanogenerator fabricated using metal organic framework composite", *Adv. Funct. Mater*., vol. 29, p. 1807655, 2019.
[52] R. M. Wen et al., "Remarkably enhanced triboelectric nanogenerator based on flexible and transparent monolayer titania nanocomposite", *Nano Energy*, vol. 50, pp. 140-147, 2018.
[53] Z. M. Lin et al., "Triboelectric nanogenerator enabled body sensor network for self-powered human heart-rate monitoring", *ACS Nano*, vol. 11, pp. 8830-8837, 2017.
[54] W. Seung et al., "Nanopatterned textile-based wearable triboelectric nanogenerator", *ACS Nano*, vol 9, pp. 3501-3509 2015
[55] L. Zhang et al., "Lawn structured triboelectric nanogenerators for scavenging sweeping wind energy on rooftops", *Adv. Mater*., vol. 28, pp. 1650-1656 2016.
[56] S. Xu et al., "Stretchable batteries with self-similar serpentine interconnect and integrated wireless recharging systems", *Nat. Commun*., vol. 4, p. 1543 2013.
[57] P. K. Yang et al., "A flexible, stretchable and shape-adaptive approach for versatile energy conversion and self-powered biomedical monitoring", *Adv. Mater*., vol. 27, pp. 3817-3824 2015.
[58] M. Vosgueritchian, D. J. Lipomi and Z. A. Bao, "Highly conductive and transparent PEDOT: PSS films with a fluoro surfactant for stretchable and flexible transparent electrodes", *Adv. Funct. Mater*., vol. 22, pp. 421-428, 2012.
[59] C. Y. Wang, W. Zheng, Z. L. Yue, C. O. Too and G. G. Wallace, "Buckled, stretchable poly pyrrole electrodes for battery applications", *Adv. Mater*., vol. 23, pp. 3580-3584, 2011.
[60] D. C. Hyun et al., "Ordered zigzag stripes of polymer gel/metal nanoparticle composites for highly stretchable conductive electrodes", *Adv. Mater*., vol. 23, pp. 2946-2950, 2011.
[61] M. Amjadi, K. U. Kyung, I. Park and M. Sitti, "Stretchable, skin-mountable, and wearable strain sensors and their potential applications: a review", *Adv. Funct. Mater*., vol. 26, pp. 1678-1698, 2016.
[62] N. Matsuhisa et al., "Printable elastic conductors with a high conductivity for electronic textile applications", *Nat. Commun*., vol. 6, p. 7461, 2015.
[63] G. D. Moon et al., "Highly stretchable patterned gold electrodes made of Au nano sheets", *Adv. Mater*. vol. 25, pp. 2707-2712, 2013.
[64] F. Yi et al., "Stretchable and waterproof self-charging power system for harvesting energy from diverse deformation and powering wearable electronics", *ACS Nano*, vol. 10, pp. 6519-6525, 2016.
[65] Y. C. Lai et al., "Electric eel skin inspired mechanically durable and super- stretchable nanogenerator for deformable power source and fully autonomous conformable electronic-skin applications", *Adv. Mater*., vol. 28, pp. 10024-10032, 2016.
[66] G. H. Lim et al., "Fully stretchable and highly durable triboelectric nanogenerators based on gold-nanosheet electrodes for self-powered human- motion detection", *Nano Energy*, vol. 42, pp. 300-306, 2017.
[67] M. D. Dickey, "Stretchable and soft electronics using liquid metals", *Adv.Mater*., vol. 29, p. 1606425, 2017.
[68] R. Matsuzaki. and K. Tabayashi, "Highly stretchable, global, and distributed local strain sensing line using GaInSn electrodes for wearable electronics", *Adv. Funct. Mater*., vol. 25, pp. 3806-3813, 2015.
[69] J. Yoon et al., "Design and fabrication of novel stretchable device arrays on a deformable polymer substrate with embedded liquid-metal interconnections", *Adv. Mater*., vol. 26, pp. 6580-6586, 2014.
[70] Y. Q. Yang et al., "Liquid metal based super-stretchable and structure design able triboelectric nanogenerator for wearable electronics", *ACS Nano*, vol. 12, pp. 2027-2034, 2018.

[71] F. Yi et al., "A highly shape-adaptive, stretchable design based on conductive liquid for energy harvesting and self-powered biomechanical monitoring", *Sci. Adv*., vol. 2, pp. 150-162, 2016.
[72] J. Shi et al., "A liquid PEDOT:PSS electrode based stretchable triboelectric nanogenerator for a portable self-charging power source", *Nanoscale*, vol. 11, pp. 7513–7519, 2019.
[73] S. Niu, X. Wang, Yi F., Y. S. Zhou, and Z. L. Wang, "A universal self-charging system driven by random biomechanical energy for sustainable operation of mobile electronics", *Nat. Commun*., vol. 6, p. 8975, 2015.
[74] X. Nan et al., "Highly efficient storage of pulse energy produced by triboelectric nanogenerator in $Li_3V_2(PO_4)3$/c cathode Li-ion batteries", *ACS Appl. Mater. Interfaces*, vol. 8, pp. 862-870, 2016.
[75] S. H. Wang et al., "Motion charged battery as sustainable flexible-power-unit", *ACS Nano*, vol. 7, pp. 11263–11271, 2013.
[76] X. L. Zhang et al., "Lithium-ion batteries: charged by triboelectric nanogenerators with pulsed output based on the enhanced cycling stability", *ACS Appl. Mater. Interfaces*, vol. 10, pp. 8676-8684, 2018.
[77] X. Liu, K. Zhao, Z. L. Wang, and Y. Yang, "Unity convoluted design of solid Li-ion battery and triboelectric nanogenerator for self-powered wearable electronics" *Adv. Energy Mater*., vol. 7, p. 1701629, 2017.
[78] X. Y. Xue, S. H. Wang, W. X. Guo, Y. Zhang, and Z. L. Wang, "Hybridizing energy conversion and storage in a mechanical to electrochemical process for self- charging power cell", *Nano Lett.*, vol. 12, pp. 5048-5054, 2012.
[79] C. I. Li et al., "Vander waal epitaxy of flexible and transparent VO_2 film on muscovite", *Chem. Mater*., vol. 28, pp. 3914-3919, 2016.
[80] S. R. Bakaul, et al., "High speed epitaxial perovskite memory on flexible substrates", *Adv. Mater*., vol. 29, p. 1605699, 2017.
[81] Z. Liang et al., "All-inorganic flexible embedded thin-film capacitors for dielectric energy storage with high performance", *ACS Appl. Mater. Interfaces*, vol. 11, pp. 5247-5255, 2019.
[82] J. Chung et al., "Capacitor-integrated triboelectric nanogenerator based on metal-metal contact for current amplification", *Adv. Energy Mater*., vol. 8, p. 1703024, 2018.
[83] Z. L. Wang, L. Lin, J. Chen, S. Niu, and Y. Zi, *Triboelectric nano-generators*. Springer International Publishing, Cham: Springer, 2016.
[84] H. Zou, et al., "Quantifying the triboelectric series", *Nat Commun*., vol. 10, p. 1427, 2019.
[85] S. Liu, W. Zheng, B. Yang, and X. Tao, "Triboelectric charge density of porous and deformable fabrics made from polymer fibers", *Nano Energy*, vol. 53, pp. 383-390, 2018.
[86] Z. L. Wang, "On the first principle theory of nanogenerators from Maxwell's equations", *Nano Energy*, vol. 68, p. 104272, 2020.
[87] Z. L. Wang, "On the first principle theory of nanogenerators from Maxwell's equations", *Nano Energy*, vol. 68, 104272, 2019.
[88] C. Yao, A. Hernandez, Y. Yu, Z. Cai, and X. Wang, "Triboelectric nanogenerators and power-boards from cellulose nanofibrils and recycled materials", *Nano Energy*, vol. 30, pp. 103-108, 2016.
[89] C. Yao, X. Yin, Y. Yu, Z. Cai, and X. Wang, "Chemically functionalized natural cellulose materials for effective triboelectric nanogenerator development", *Adv Funct Mater*., vol. 27, p. 1700794, 2017.
[90] S. Kim, M. K. Gupta, K. Y. Lee, et al., "Transparent flexible graphene triboelectric nanogenerators", *Adv Mater*., vol. 26, pp. 3918-3925, 2014.
[91] C. Wu, T. W. Kim, J. H. Park, et al., "Enhanced triboelectric nanogenerators based on MoS_2 monolayer nanocomposites acting as electron-acceptor layers", *ACS Nano*., vol. 11, pp. 8356-8363, 2017.
[92] M. Seol, S. Kim, Y. Cho, et al., "Triboelectric series of 2D layered materials", *Adv Mater*., vol. 30, p. 1801210, 2018.
[93] S. Wang, L. Lin, Y. Xie, Q. Jing, S. Niu and Z. L. Wang, "Sliding- triboelectric nanogenerators based on in-plane charge- separation mechanism", *Nano Lett*., vol. 13, pp. 2226-2233, 2013.
[94] Y. Xie, S. Wang, L. Lin, et al., "Rotary triboelectric nanogenerator based on a hybridized mechanism for harvesting wind energy", *ACS Nano*., vol. 7, pp. 7119-7125, 2013.
[95] W. Tang, C. B. Han, C. Zhang, and Z. L. Wang, "Cover sheet based nanogenerator for charging mobile electronics using low- frequency body motion/vibration", *Nano Energy*, vol. 9, pp. 121-127, 2014.
[96] J. Chen, X. Pu, H. Guo, et al., "A self-powered 2D barcode recognition system based on sliding mode triboelectric nanogenerator for personal identification", *Nano Energy*., vol. 43, pp. 253-258, 2018.
[97] J. Wang, W. Ding, L. Pan, et al., "Self-powered wind sensor system for detecting wind speed and direction based on a triboelectric nanogenerator", *ACS Nano*., vol. 12, pp. 3954-3963, 2018.
[98] R. Zhang, M. Hummelgård, J. Ortegren, et al., "Human body constituted triboelectric nanogenerators as energy harvesters, code transmitters, and motion sensors", *ACS Appl Energy Mater*., vol. 1, pp. 2955-2960 2018.
[99] S. Wang, L. Lin, Y. Xie, Q. Jing, S. Niu, and Z. L. Wang, "Sliding- triboelectric nanogenerators based on in-plane charge- separation mechanism", *Nano Lett*., vol. 13, pp. 2226-2233, 2013.

[100] Y. Xie, S. Wang, S. Niu, et al., "Grating structured freestanding triboelectric layer nanogenerator for harvesting mechanical energy at 85% total conversion efficiency", *Adv Mater*., vol. 26, pp. 6599-6607, 2014.
[101] T. Liu, M. Liu, S. Dou, et al., "Triboelectric nanogenerator based soft energy-harvesting skin enabled by toughly bonded elastomer/hydro gel hybrids", *ACS Nano*., vol. 12, pp. 2818-2826, 2018.
[102] A. Ahmed, Z. Saadatnia, I. Hassan, et al., "Self-powered wireless sensor node enabled by a duck-shaped triboelectric nanogenerator for harvesting water wave energy", *Adv Energy Mater*., vol. 7, p. 1601705, 2017.
[103] H. Zou, Y. Zhang, L. Guo, et al., "Quantifying the triboelectric series", *Nat. Commun*., vol. 10, p. 1427, 2019.
[104] J. P. Lee, J. W. Lee and J. M. Baik, "The progress of PVDF as a functional material for triboelectric nanogenerators and self – powered sensors", *Micromachines*, vol. 9, pp. 1-13, 2018.